Spectroscopy of ^{9}B via high-resolution ejectile-tagged recoil break-up

Wheldon, C.; Kokalova Wheldon, Tzanka; Freer, M.; Walshe, J.; Hertenberger, R.; Wirth, H. F.; Ashwood, N. I.; Barr, M.; Curtis, N.; Faestermann, Th; Lutter, R.; Malcolm, J. D.; Marín-Lámbarri, D. J.

DOI:
10.1103/physrevc.91.024308

Spectroscopy of ^{9}B via high-resolution ejectile-tagged recoil break-up

C. Wheldon,[1,*] Tz. Kokalova,[1] M. Freer,[1] J. Walshe,[1] R. Hertenberger,[2] H.-F. Wirth,[2] N. I. Ashwood,[1] M. Barr,[1] N. Curtis,[1] Th. Faestermann,[3] R. Lutter,[2] J. D. Malcolm,[1] and D. J. Marín-Lámbarri[1]

[1]*School of Physics and Astronomy, University of Birmingham, Edgbaston, Birmingham B15 2TT, United Kingdom*

[2]*Fakultät für Physik, Ludwig-Maximilians-Universität München, D-85748 Garching, Germany*

[3]*Physik Department, Technische Universität München, D-85748 Garching, Germany*

(Received 17 December 2014; published 11 February 2015)

An experiment has been carried out using the ^{9}Be(^{3}He, t)^{9}B* reaction at a beam energy of 33 MeV. A large acceptance silicon-strip array was used to detect the ^{9}B* break-up in coincidence with the triton ejectiles in the high-resolution Munich-Q3D spectrograph. The excitation energy regime <3 MeV has been explored and the spectrum resulting from proton decaying states, isolated and characterized. Additional resonance strength is observed at 1.86 MeV ±70 keV(stat) ±35 keV(syst), in agreement with two other recent measurements at higher energies and different angles. The consequences for the "missing" $^{1}/_{2}^{+}$ first excited state are discussed. Additionally, the branching ratios for the 2.36 MeV $^{5}/_{2}^{-}$ state have been measured as $\Gamma_{\alpha 0}/\Gamma = 0.98 \pm 0.12$ and $\Gamma_{p0}/\Gamma = 0.016 \pm 0.008$, in close agreement with earlier work.

DOI: 10.1103/PhysRevC.91.024308 PACS number(s): 21.10.−k, 24.10.Lx, 25.55.Hp, 27.20.+n

I. INTRODUCTION

Mirror pairs of nuclei provide information about the charge independence of the nuclear force. Though many such pairs have been investigated and are well understood, there remains the longstanding mystery of the $^{9}_{4}$Be$_{5}$/$^{9}_{5}$B$_{4}$ mirror pair, concerning the observation of the $^{1}/_{2}^{+}$, first excited state in ^{9}B that as yet remains to be conclusively observed. The corresponding level in the mirror partner, ^{9}Be, lies at 1.684(7) MeV with a total width of 217(10) keV [1], comprising approximately 100% neutron decay to ^{8}Be which itself subsequently decays into two α particles. The nature of the ^{9}Be state could be either clustered (two-α particles bound by a covalent σ-type neutron) or shell-model-like (^{8}Be core + neutron in the *sd* shell). These two configurations have very different sizes, with the latter corresponding to the more compact structure. The Coulomb energy is very sensitive to the volume occupied by the valence particle, which translates into excitation energy with respect to the ground state. Importantly, measuring the excitation energy of the $^{1}/_{2}^{+}$ state in ^{9}B allows the Coulomb energy difference (CED) for this mirror pair to be determined and the nature of these states to be established. Thus, there is significant interest in forming a complete spectroscopic picture of the low-lying energy region of ^{9}B. Given the implications of the properties of the $^{1}/_{2}^{+}$ resonance and that nine-nucleon systems are calculable in *ab initio* approaches it remains as important as ever to resolve this longstanding enigma of ^{9}B's first excited state.

Establishing the excitation energy of the mirror $^{1}/_{2}^{+}$ level would also provide discriminating data for the many existing theoretical calculations. A good summary is given in Ref. [2]. Recently, Barker [3] used a modified version of the potential model from Ref. [4] to calculate the excitation energy based on the configuration of the 0_{2}^{+} states in ^{10}Be and ^{10}B, obtaining two possible values of $E_{x}(^{9}\mathrm{B})$=1.36 and 1.74 MeV, compared to Fortune and Sherr's original value of 1.31 MeV [4]. Arai and coworkers [5], using a microscopic multicluster model predicted the $^{1}/_{2}^{+}$ at around 1.2 MeV, with a large width of about 3 MeV. It is apparent that the variation in calculations matches that of the measurements, from which, since the discovery of ^{9}B in 1940 [6,7], the $^{1}/_{2}^{+}$ excited state has been reported somewhere between 0.8 and 1.8 MeV [1,8,9].

The experimental search is complicated by the strongly populated $^{5}/_{2}^{+}$ state at 2.788(30) MeV (Γ = 550(40) keV [1] and $\Gamma_{p}/\Gamma \approx 100\%$ [10]) and a broad $^{1}/_{2}^{-}$ state at 2.75(30) MeV (Γ = 3.13(20) MeV, $\Gamma_{p}/\Gamma \geqslant 90\%$ [1]). One of the issues with earlier studies is the poor energy resolution and the absence of background-free channel selection for the ejectile or recoil. Here, investigations of ^{9}B via charge exchange using a charged-particle array in coincidence with the high-resolution Munich Q3D spectrograph are reported for the low-excitation energy region.

II. EXPERIMENTAL METHOD

The ^{9}Be(^{3}He,t)^{9}B reaction [Q= −1.087(1) MeV] was used at a bombarding energy of 33 MeV on a self-supporting ^{9}Be target. The ^{9}Be target thickness was measured to be 203(7) μg/cm^{2} using the energy loss of α particles from a Pu-Am-Cm triple-α source. The beam was provided by the Maier Leibnitz Laboratory 15 MV tandem Van de Graaff accelerator of the Technische and Ludwig-Maximilians Universität, Munich. The triton ejectiles were focused by the Q3D spectrograph [11] at 30° on to a position-sensitive proportional counter [12,13] situated at the focal plane. Energy-loss (via an initial cathode foil and horizontal anode wires preceding the position sensitive cathode strip foil) and energy (via a plastic scintillator after the cathode strips) were also recorded enabling identification of the ejectile, whereas position along the focal plane is related to the excitation energy of the ^{9}B recoil, independent of angle. The position scale was calibrated using known narrow states in ^{9}B, as well as ^{19}Ne and ^{7}Be from (^{3}He,t) reactions on ^{6}LiF and $^{\mathrm{nat}}$LiF targets. The Birmingham large angular acceptance

*Corresponding author: c.wheldon@bham.ac.uk

charged-particle array was placed inside the Q3D chamber, and comprised four double-sided silicon strip detectors each measuring 50×50 mm^2 with 16 strips on each face; the strips being mutually orthogonal on the front and back faces. The detectors were located in pairs inside the chamber at in-plane centre angles of 62° and 152° with respect to the beam axis with one detector in each pair above and one below the reaction plane. The forward detectors were situated at 87 and 81 mm from the target and the backward pair at 73 and 67 mm. The triple-α source provided the silicon-detector calibration points, for which a resolution of ≈55 keV was achieved.

Short set-up runs at Q3D settings of 0.0 MeV and 1.00–1.50 MeV (these ^{9}B excitation energies corresponding to a nominal point approximately 60% along the focal plane) were used for which the silicon-detectors were excluded. The majority of the coincidence data collected were with the Q3D set at an excitation energy, $E_x = 1.450$ MeV, which, due to the highly dispersive nature of the Q3D, corresponds to a range of 0.48–2.70 MeV. Additionally, a small amount of data were obtained at E_x=2.650 MeV. The master trigger in both cases was a "good" Q3D event (a coincidence between the Q3D scintillator and a horizontal wire, i.e., a Q3D singles trigger), initiating the readout of all the ADCs, including the silicon detectors, with a gate length of 5 μs.

III. ANALYSIS AND RESULTS

The data analysis consisted of several key steps. The first is the event-by-event Gaussian fitting of the focal-plane charge distributions [14] to obtain the ^{9}B excitation energy and use of the Q3D energy and energy-loss data to select triton ejectiles. Events passing this stage were further processed for silicon-detector hits via the application of upper and lower thresholds set individually for each strip (typically between 0.9–5.0 MeV for ^{9}B events), and by matching front and back energies. Immediately prior to the front-back matching, corrections were applied for charge sharing (hits in two neighboring strips on one detector face with an energy sum equal to a single hit on the opposing face) due to hitting the interstrip region, pile-up (multiple hits in a strip on one detector face) and for front contact hits (a particle hitting the front contact causing an event on the front face, with no corresponding event in the back face). These latter are removed such that other hits in the same event can be processed normally.

The resulting energies across all detectors were subsequently corrected for energy loss in the target by assuming that the particles corresponded to α particles and protons as required. Finally, the multiplicity-two and -three events were processed with the majority being two-hit events. This final step involved a kinematic reconstruction, by initially assuming the two highest energy hits were α particles. Under this premise, the ^{8}Be excitation energy was calculated as

$$E_x(^8\mathrm{Be}) = \sum_{i=1}^{2} E_i - \frac{1}{2m(^8\mathrm{Be})} \sum_{j=x,y,z} \{p_1(j) + p_2(j)\}^2, \quad (1)$$

where $p_i(x,y,z)$ are the momentum components of the ith detected particle, calculated from the measured energy, E_i, and angle information together with the mass from assuming its identity. The resulting spectrum is shown in Fig. 1(black stepped line).

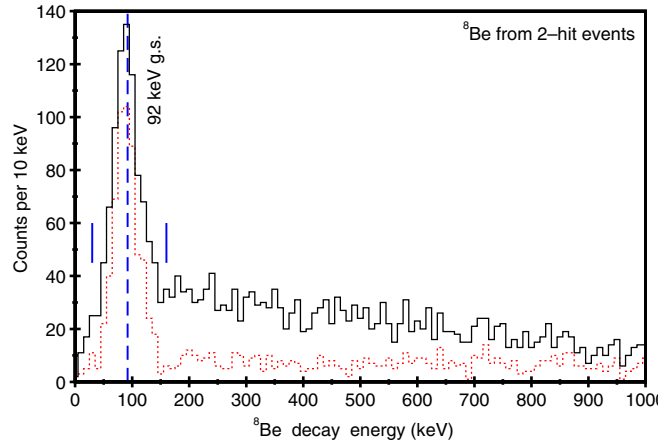

FIG. 1. (Color online) Spectrum showing the reconstructed ^{8}Be spectrum for multiplicity-two events assuming two detected α particles (black stepped line). The red dotted spectrum shows the effect of two additional selection criteria: on the proton distribution in a Catania plot (see text and Fig. 2 for details) and requiring both hits at forward angles. The ^{8}Be ground state is clearly visible at 92 keV (blue dashed line) in both cases. The vertical continuous blue lines are the limits used to select the events.

The next stage involved calculating the energy of the postulated missing proton via

$$E_p = \frac{p_p^2}{2m(p)} = \frac{1}{2m(p)} \sum_{j=x,y,z} \{p_b(j) - p_t(j) - p_1(j) - p_2(j)\}^2 \quad (2)$$

where b, p, and t refer to the beam, protons, and tritons, respectively. The reaction Q value can then be determined from

$$Q = E_t + E_1 + E_2 + \frac{p_p^2}{2m(p)} - E_b. \quad (3)$$

From rearranging Eq. (3), it can be seen that constructing a two-dimensional (2-D) plot of $p_p^2/2$ against $E_b - E_t - E_1 - E_2$ will lead to the proton distribution having a gradient of $1/m(p)$ and an intercept of $-Q$; a Catania plot, as shown in Fig. 2.

The analysis procedures were informed throughout by comparison with Monte Carlo simulations using the RESOLUTION8 code (for more information see Refs. [15,16]). The simulations indicated that α particles are only detected at forward angles and that the contamination by events from the competing ^{5}Li + α channel could be reduced via a 2-D gate around predominantly proton events in the Catania plot. The effect of these cuts can be seen in Fig. 1(red), demonstrating significant background reduction.

The events in the ^{8}Be ground-state peak were selected and the resulting Q-value distribution is shown in Fig. 3(red). The peak obtained is close to the expected value of $Q = -0.810$ MeV from atomic masses [17]. For the remaining events, the Q3D focal-plane spectra were analyzed

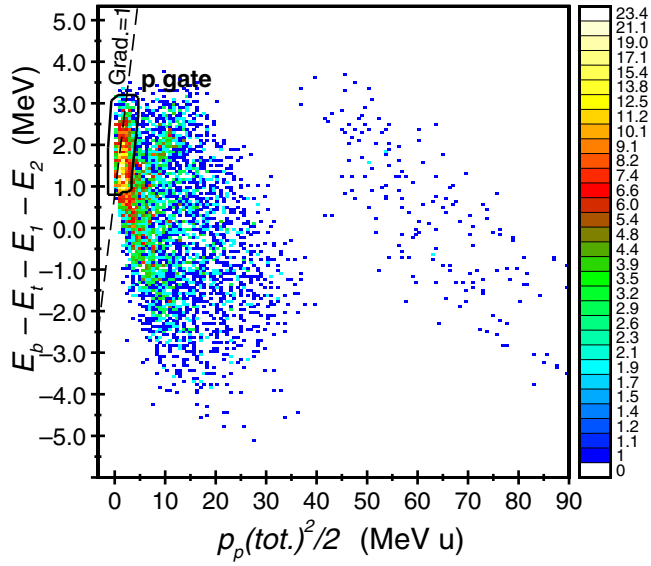

FIG. 2. (Color online) Catania plot used to reduce the background in the proton-gated spectra (see text for details). The dashed line indicates where $m = 1$ (i.e., proton) events would lie with a Q value of -0.810 MeV. The proton locus is skewed by the presence of ^{5}Li events. The gate used to select predominantly proton events is also illustrated and was obtained from simulations.

together with the data from a corresponding treatment of the multiplicity-three events yielding the total spectrum as shown in Fig. 4(black stepped line). This can be contrasted with the spectrum obtained when gating on the background in Fig. 1, as shown in Fig. 4(red). The robustness of the event selection is clear; the proton channel using the ^{8}Be ground state [Fig. 4(black stepped line)] suppresses the $^{5}/_{2}^{-}$ state at 2.36 MeV the decay of which is dominated by the ^{5}Li + α channel, $\Gamma_{\alpha}/\Gamma = 0.99$ [10]. To compare the quantitative agreement between the current and published data, the branching ratio of the 2.36 MeV resonance was extracted

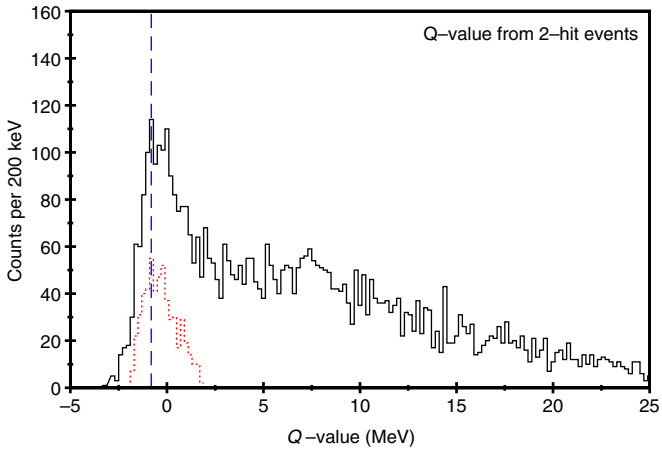

FIG. 3. (Color online) Plot of the reconstructed Q value obtained with no gates (black stepped line) and following the background-suppressed ^{8}Be selection (red dotted line). The dashed blue line is the calculated Q value.

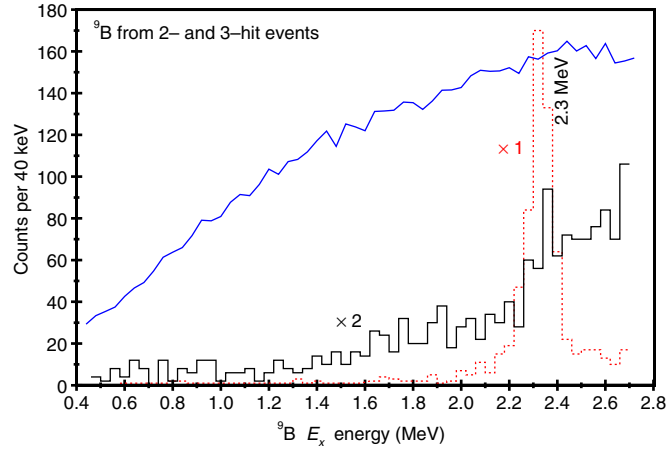

FIG. 4. (Color online) Boron-9 excitation energy spectrum from the Q3D focal-plane detector gated by decay through the ^{8}Be ground state for multiplicities two and three (black stepped line). The red dotted line is gated by the background in the ^{8}Be spectrum of Fig. 1(red). The blue continuous line represents the *relative* detection and reconstruction efficiency for the two-hit ^{8}Be events.

using

$$\frac{\Gamma_\alpha}{\Gamma} = \frac{I(\alpha)}{I(\mathrm{tot})\epsilon_\alpha} \quad \text{and} \quad \frac{\Gamma_p}{\Gamma} = \frac{I(p)}{I(\mathrm{tot})\epsilon_p}, \tag{4}$$

where ϵ_α and ϵ_p are the total efficiencies for selecting events in the ^{5}Li + α and ^{8}Be + p channels, respectively, obtained from Monte Carlo–generated events, sorted with the same analysis code as used for the data. The ratio of α-channel events, $I(\alpha)$, in the Si-gated spectrum to the total number of α-channel events in the Q3D, $I(\mathrm{tot})$, gives the efficiency. A similar efficiency can be obtained for the proton-decay channel. The results are $\Gamma_{\alpha 0}/\Gamma = 0.98 \pm 0.12$ ($\epsilon_\alpha = 2.2\%$) and $\Gamma_{p0}/\Gamma = 0.016 \pm 0.008$ ($\epsilon_p = 3.7\%$). (Note that the proton branch is consistent with zero at two standard deviations.) The relatively large uncertainties are due to the sensitivity of the events to the lower Si-detector thresholds, leading to the ratios being extracted at higher thresholds, reducing the statistics and leading to a corresponding increase in the uncertainties. For the proton channel there is an additional background subtraction from the ^{5}Li + α channel lying under the ^{8}Be$_{g.s.}$ peak as seen in Fig. 1(red). Both branching ratios are in close agreement with those of Gete *et al.* [10].

IV. DISCUSSION

Before commenting on the implications of the current data for the $^{1}/_{2}^{+}$ state, a summary of the properties of the established states below 6 MeV is given in Table I, as contributions from these states can be critical to the interpretation of the data.

The effect of energy straggling in the thick target was characterized using the known properties of the 2.36 MeV $^{5}/_{2}^{-}$ state with $\Gamma = 81(5)$ keV. A Voigt profile [19] was fitted to Fig. 4(red) indicating a resolution of 41(13) keV for the FWHM of the Gaussian component of the Voigt function. This fit is shown in Fig. 5. All subsequent fits use a Voigt line shape with the Gaussian component fixed at FWHM=41 keV.

TABLE I. A summary of the properties of the established states < 6 MeV in ^{9}B from the most recent tabulation [1].

E_{level} [MeV±(keV)]	I^{π}	Γ_{tot} [keV]	$\Gamma_{\alpha}/\Gamma_{\text{tot}}$ ^{5}Li$_{\text{g.s.}}$	$\Gamma_{p}/\Gamma_{\text{tot}}$ ^{8}Be$_{\text{g.s.}}$
0	$\frac{3}{2}^{-}$	0.54(21)	–	1.00
2.361±5	$\frac{5}{2}^{-}$	81(5)	0.99(19)[a]	0.005(6)[a]
2.75±300	$\frac{1}{2}^{-}$	3130(200)	0.10(1)[a]	0.90(9)[a]
2.788±30	$\frac{5}{2}^{+}$	550(40)	–	0.90
4.3±200[b]	–	1600(200)	–	–

[a]Branching ratios taken from Ref. [10].
[b]According to Ref. [1], this state is reported in Ref. [18] from the ^{9}Be(p,n) reaction.

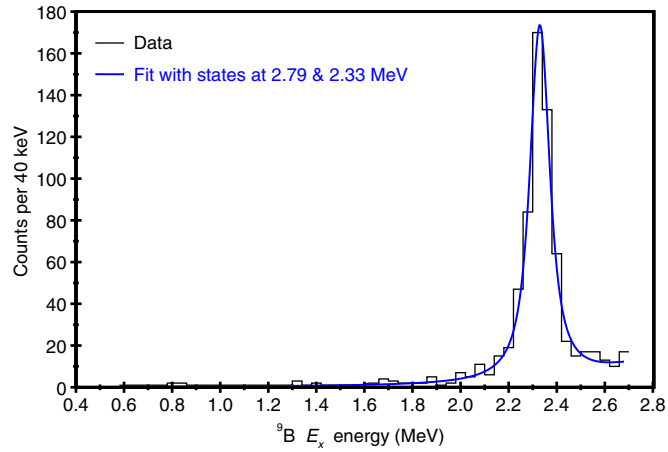

FIG. 5. (Color online) Data for the ^{5}Li + α channel (black stepped line). These data were used to constrain the Gaussian FWHM for the Voigt profiles by fitting a Voigt profile (continuous blue line) to the 2.3 MeV state using its known width, $\Gamma = 81(5)$ keV [1] for the Lorentzian component.

The centroid obtained, 2.330 MeV ±3 keV(stat), is consistent with the systematic energy uncertainty of ±35 keV obtained from the Q3D calibration fitting procedure.

Figure 6 shows the spectrum fitting for ^{8}Be-gated ^{9}B data. The fits were performed by using the known centroid and width data [1] for the 2.36 and 2.79 MeV states. Using only these two resonances results in the red dashed line in Fig. 6(b). However, there is an excess of counts in the 1.8 MeV region, and the subsequent χ^2 minimization results in a state at 1.86 MeV ±70 keV(stat) ±35 keV(syst) (solid blue line in Fig. 6) with a width of $\Gamma = 650(160)$ keV, the latter corresponding to the Lorentzian width component of the Voigt function. No such excess is evident in the ^{5}Li-gated spectrum (Fig. 5), consistent with the ^{5}Li + α threshold lying at 1.688 MeV and the expected suppression at energies near threshold due to the barrier penetrabilities; the barrier penetrabilities for a $1/2^{+}$ state at 1.8 MeV are $P_{\alpha} = 7.42 \times 10^{-9}$ and $P_{p} = 0.70$—a factor of 9.4×10^{7} favoring proton decay. Note that these calculations do not take account of the ^{5}Li ground-state width of $\Gamma = 1.23$ MeV [20] which decreases the overall penetrability factor, though not by seven orders of magnitude. It is therefore expected that any state at (or below) 1.9 MeV will decay almost exclusively via proton emission, independent of the spin of the level.

During the analysis, possible sources of background in the proton spectrum, other than α events from ^{9}B, were explored. Taking the three final-state particles of t, p, and ^{8}Be, a ^{11}B state is conceivable ($t + {}^{8}$Be). However, the large negative Q value of −11.224 MeV for $^{11}\text{B} \rightarrow {}^{8}\text{Be} + t$ leads to ^{11}B excitation energies > 29 MeV following reconstruction and does not contribute. Similarly, for $^{4}\text{He} \rightarrow t + p, Q = -19.814$ MeV.

Finally, an upper limit on the contribution from the known, wide, 2.75 MeV state with $\Gamma = 3.13$ MeV has been tested, shown by the red dotted line of Fig. 6(b). This is found to be small and can clearly not account for all of the counts close to 1.8 MeV. It was not possible to independently establish the

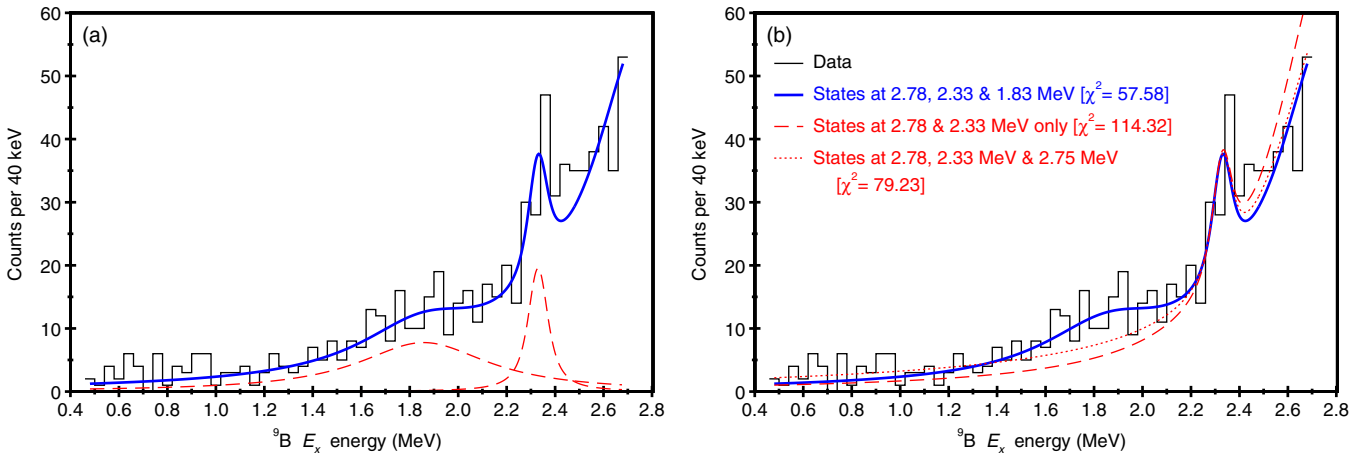

FIG. 6. (Color online) Data (black stepped line) for the ^{8}Be + p channel. (a) shows the best fit to the data (thick smooth blue line), obtained by inclusion of a third state at 1.86(7) MeV [$\Gamma = 650(160)$ keV]. The two known levels at 2.75 and 2.3 MeV have also been included in the fit. The individual components of the 2.3 and 1.86 MeV states are shown by dashed red lines. In (b) the same blue line of best fit is compared to a fit excluding the 1.86 MeV state (red dashed line). The red dotted line also excludes the 1.86 MeV level, but additionally includes the very broad state at 2.75 MeV [$\Gamma = 3.13(20)$ MeV]. Values for χ^2 are quoted in square brackets.

precise contributions from such states due to the extremely low statistics in the gated spectra obtained using the 2650 keV Q3D setting.

In order to investigate possible interference effects between the final states, an R-matrix analysis was performed using the AZURE2 code [21] with incoming and outgoing channels of $p + {}^{8}$Be and $p + {}^{8}$Be*[0.001 MeV], respectively, and a channel radius of 3.75 fm (i.e., $r_0 = 1.25$ fm). The small inelastic excitation in the outgoing channel enables the Coulomb interaction to be switched off. States with $I^{\pi} = 1/2^{+}$, $E_x = 1.860$ MeV, $\Gamma = 650$ keV and $I^{\pi} = 5/2^{+}$, $E_x = 2.788$ MeV, $\Gamma = 365$ keV have been included. The narrow $5/2^{+}$ state close to 2.3 MeV has been omitted as its intensity in the proton channel is consistent with zero at two standard deviations. The centroid positions in the excitation spectrum were investigated in order to quantify the interference effects. This study was made with all combinations of interference polarity between the two states and in each of these cases over a large range of angles. A representative spectrum is shown by the dashed red in Fig. 7. As can be seen, the centroids of the included states are not shifted by interference effects. What was observed in this analysis is that there is little energy dependence on angle regardless of the sign of the interference.

Examining other recent studies that have employed this charge-exchange reaction, in 2001 Akimune and coworkers [22] fitted the 0° triton spectrum following reactions at 150 MeV/A, and reported a newly observed state at $1.80^{+0.22}_{-0.16}$ MeV with $\Gamma = 600^{+300}_{-270}$ keV. These properties overlap within one standard deviation with those reported here. More recently, the (^{3}He,t) reaction at 140 MeV/A was measured at 0° with a resolution of 30 keV by Scholl *et al.* [23] in which a candidate state in the spectrum fitting at 1.850 ± 0.130 MeV with $\Gamma = 700^{+270}_{-200}$ keV was reported; extremely close to that of Ref. [22] and the current work. This provides some level of consistency, as both Refs. [23] and [22] were measured at 0° whereas the current work was centered at 30° and used a significantly lower beam energy. A weighted average of the current results with those of Refs. [22,23] yields a centroid of 1.85 ± 0.06 MeV and $\Gamma = 650 \pm 125$ keV.

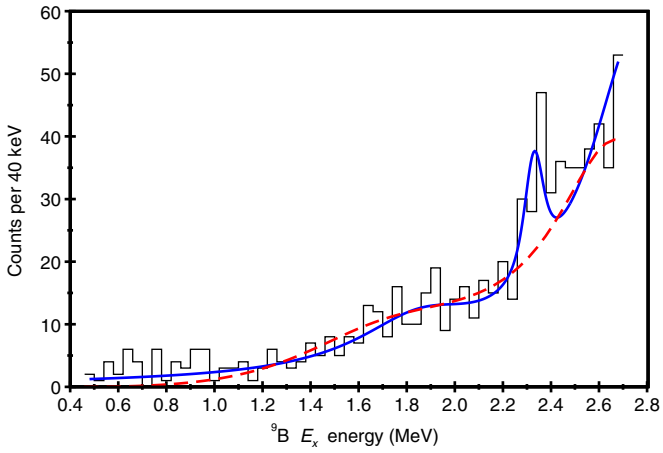

FIG. 7. (Color online) Here, the data (black stepped line) for the ^{8}Be + p channel and Voigt fit (thick smooth blue line) are compared to a representative R-matrix calculation corresponding to 20° (red dashed line) in order to investigate interference effects. See text for details.

A more global examination of the experimental studies is revealed in the most recent compilation from 2004 which gives the approximate centroid from a large range of studies as ≈1.6 MeV [1] and this has remained unchanged over the three preceding compilations [24–26] dating back to 1979, though in the earlier volumes, a width was also quoted of $\Gamma \approx 700$ keV. The value of 1.86(7) MeV here lies only 16% (260 keV) higher in excitation energy, and with a comparable width. In contrast, a recent detailed, though complicated analysis of ^{9}B data is that by Baldwin *et al.* [2] using the ^{6}Li + ^{6}Li reaction at 60 MeV. The properties of the $1/2^{+}$ candidate state were reported as 0.8–1.0 MeV with Γ≈1.5 MeV, significantly lower in energy than that suggested in the current work. Different reactions seem to consistently report resonance strength at different excitation energies. While it is tempting to attribute this to the existence of more than one state, such a scenario is unlikely due to the absence of a missing analog in ^{9}Be. Returning to Baldwin's study, it is also interesting as it suggests that the population mechanism using ^{6}Li is via ^{6}Li(^{6}Li,d)^{10}B, followed by sequential neutron emission, rather than the direct ^{6}Li(^{6}Li,t)^{9}B process. This offers a possible route for future studies of ^{9}B. Fortune and Sherr [9] suggest an alternative approach, via the $\Gamma = 380$ keV $1/2^{+}$ resonance at 11.86 MeV in ^{13}N using the ^{12}C(p,α)^{9}B reaction. This latter approach, also has the advantage of comparing on and off-resonance measurements to quantify background contributions.

An excitation energy of 1.86 MeV for the $1/2^{+}$ resonance, implies that the exchange of a neutron for a proton has a significant effect, increasing the energy with respect to the $3/2^{-}$ ground state by ≈180 keV compared to ^{9}Be. Given the assumption of identical wave functions for the underlying structure of such mirror states, the principal way to induce such a shift following charge exchange is via a compact configuration. This would support the shell-model-like scenario of a ^{8}Be core + neutron, for the analog state in ^{9}Be, rather than the enhanced, covalently-bound α structure. However, in order make a quantitative comparison with the precise magnitude of this shift and the structure described by the underlying wave function, theoretical input is needed.

V. SUMMARY

The low-lying excitation region of ^{9}B has been studied using the high-resolution Q3D spectrograph to measure the triton ejectiles following the charge-exchange reaction, ^{9}Be(^{3}He,t)^{9}B* at 33 MeV. The ^{9}B* break-up products were simultaneously measured in a large acceptance position-sensitive silicon detector array and the originating states reconstructed and filtered using kinematics. The partial decay widths of the 2.36 MeV state were measured, in agreement with earlier work, proceeding almost exclusively via the ^{5}Li + α channel; ($\Gamma_{\alpha 0}/\Gamma = 0.98 \pm 0.12$ and $\Gamma_{p0}/\Gamma = 0.016 \pm 0.008$). By selecting proton-emission events, evidence for a state at 1.86(7) MeV with $\Gamma = 650(150)$ keV was obtained. When taken together with other recent results, a weighted average yields an excitation energy of 1.85 ± 0.06 MeV and a width, $\Gamma = 650 \pm 125$ keV.

ACKNOWLEDGMENTS

It is a pleasure to thank the accelerator operators of Maier-Leibnitz Laboratory for providing a stable ^{3}He beam. We acknowledge the financial support of the UK Science and Technology Facilities Council (STFC) and the DFG Cluster of Excellence 153, 'Origin and Structure of the Universe'. Tz.K. is grateful for a Daphne Jackson grant funded by the STFC.

[1] D. R. Tilley, J. H. Kelley, J. L. Godwin, D. J. Millener, J. E. Purcell, C. G. Sheua, and H. R. Weller, Nucle. Phys. A **745**, 155 (2004).
[2] T. D. Baldwin *et al.*, Phys. Rev. C **86**, 034330 (2012).
[3] F. C. Barker, Phys. Rev. C **79**, 017302 (2009).
[4] H. T. Fortune and R. Sherr, Phys. Rev. C **73**, 064302 (2006).
[5] K. Arai, P. Descouvemont, D. Baye, and W. N. Catford, Phys. Rev. C **68**, 014310 (2003).
[6] M. Thoennessen, At. Data Nucl. Data Tables **98**, 43 (2012).
[7] R. O. Haxby, W. E. Shoupp, W. E. Stephens, and W. H. Wells, Phys. Rev. **58**, 1035 (1940).
[8] R. Sherr and H. T. Fortune, Phys. Rev. C **70**, 054312 (2004).
[9] H. T. Fortune and R. Sherr, Nucl. Phys. A **898**, 78 (2013).
[10] E. Gete *et al.*, Phys. Rev. C **61**, 064310 (2000).
[11] M. Löffler, H. J. Scheerer, and H. Vonach, Nucl. Instrum. Methods **111**, 1 (1973).
[12] H.-F. Wirth, H. Angerer, T. von Egidy, Y. Eisermann, G. Graw, and R. Hertenberger, Beschleunigerlaboratorium München, Annual Report (2000), p. 71.
[13] H.-F. Wirth, Ph.D. thesis, Technical University, München (2001), see http://tumb1.biblio.tu-muenchen.de/publ/diss/ph/2001/wirth.html.
[14] C. Wheldon, http://www.wheldon.talktalk.net/files/munich_decoder.c (2008).
[15] N. Curtis *et al.*, Phys. Rev. C **51**, 1554 (1995).
[16] N. Curtis *et al.*, Phys. Rev. C **53**, 1804 (1996).
[17] G. Audi, A. H. Wapstra, and C. Thibault, Nucl. Phys. **729**, 337 (2003).
[18] B. Pugh, Ph.D. thesis, MIT, 1985.
[19] John A. Gubner, J. Phys. A: Math Gen. **27**, L745 (1994).
[20] D. R. Tilley, C. M. Cheves, J. L. Godwin, G. M. Hale, H. M. Hofmann, J. H. Kelley, C. G. Sheu, and H. R. Weller, Nucl. Phys. A **708**, 3 (2002).
[21] R. E. Azuma, E. Uberseder, E. C. Simpson, C. R. Brune, H. Costantini, R. J. de Boer, J.Görres, M. Heil, P. J. LeBlanc, C. Ugalde, and M. Wiescher, Phys. Rev. C **81**, 045805 (2010).
[22] H. Akimune, M. Fujimura, M. Fujiwara, K. Hara, T. Ishikawa, T. Kawabata, H. Utsunomiya, T. Yamagata, K. Yamasaki, and M. Yosoi, Phys. Rev. C **64**, 041305(R) (2001).
[23] C. Scholl *et al.*, Phys. Rev. C **84**, 014308 (2011).
[24] F. Ajzenberg-Selove, Nucl. Phys. A **490**, 1 (1988).
[25] F. Ajzenberg-Selove, Nucl. Phys. A **413**, 1 (1984).
[26] F. Ajzenberg-Selove, Nucl. Phys. A **320**, 1 (1979).